Interfacial Shear Strength Estimates of NiTi - Al Matrix Composites Fabricated via Ultrasonic Additive Manufacturing

Adam Hehr, Joshua Pritchard, Marcelo J. Dapino

Smart Vehicle Concepts Center, Department of Mechanical and Aerospace Engineering,
The Ohio State University, Columbus, OH, USA, 43210

ABSTRACT

The purpose of this study is to understand and improve the interfacial shear strength of metal matrix composites fabricated via very high power (VHP) ultrasonic additive manufacturing (UAM). VHP-UAM NiTi-Al composites have shown a dramatic decrease in thermal expansion compared to Al, yet thermal blocking stresses developed during thermal cycling have been found to degrade and eventually cause interface failure. Consequently, to improve understanding of the interface and guide the development of stronger NiTi-Al composites, the interface strength was investigated through the use of single fiber pullout tests. It was found that the matrix yielded prior to the interface breaking since adhered aluminum was consistently observed on all pullout samples. Additionally, measured pullout loads were utilized as an input to a finite element model for stress and shear lag analysis, which, in turn showed that the Al matrix experienced a peak shear stress near 230 MPa. This stress is above the Al matrix's ultimate shear strength of 150-200 MPa, thus this large stress corroborates with matrix failure observed during testing. The influence of various fiber surface treatments on bond mechanisms was also studied with scanning electron microscopy and energy dispersive X-ray spectroscopy.

Keywords: ultrasonic additive manufacturing, ultrasonic consolidation, nickel titanium, shape memory alloy, interfacial shear stress, composite material, characterization

1. PROBLEM STATEMENT AND INTRODUCTION

Ultrasonic additive manufacturing (UAM) is a recently developed rapid prototyping process where thin foils of similar or dissimilar metals are ultrasonically welded together in a layer by layer process to form gap-less, 3D metal parts.[1] Along with welding, periodic machining is utilized during the UAM process to implement complex designs, features, and to remove material for embedding various objects into the structure, such as reinforcing fibers. Due to the physics of ultrasonic welding, metallic bonding takes place at temperatures far below metallic melting temperatures. Thus, temperature sensitive metals or components can be combined or built into metallic structures, like nickel titanium (NiTi) shape memory alloys. Very high power ultrasonic additive manufacturing (VHP-UAM) is a recent improvement in the UAM process where the ultrasonic weld power and down force have increased nearly an order of magnitude relative to early UAM processes. This increase in weld power and down force remedies poor interfacial properties observed in early UAM processes.[2] A schematic of the VHP-UAM process is shown in Figure 1.

Further author information: (Send correspondence to M.J.D)
A.H.: E-mail: hehr.7@osu.edu
M.J.D.: E-mail: dapino.1@osu.edu

Industrial and Commercial Applications of Smart Structures Technologies 2014,
edited by Kevin M. Farinholt, Steven F. Griffin, Proc. of SPIE Vol. 9059, 905906
 · doi: 10.1117/12.2046317

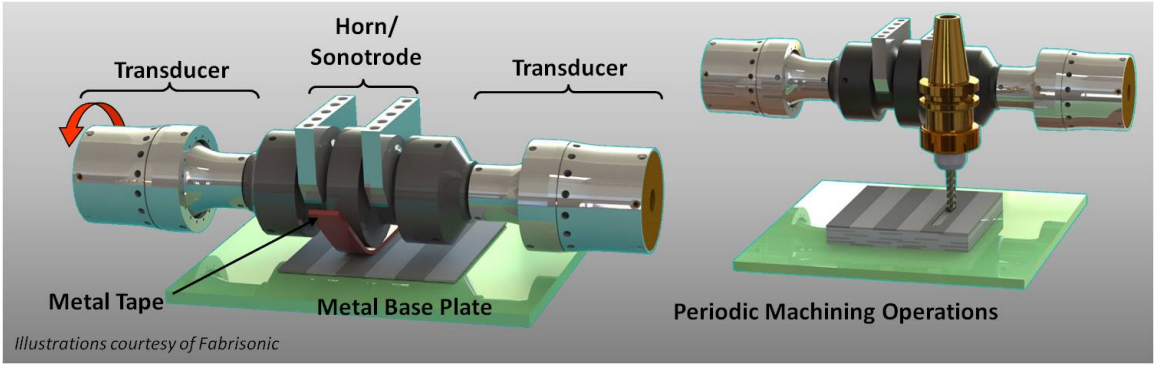

Figure 1. Ultrasonic additive manufacturing process for developing novel and unique metal composites and designs.

Recently, VHP-UAM has been utilized for fabrication of aluminum matrix composites with embedded NiTi shape memory alloy fibers for thermal expansion control applications. Specifically, when the composite is heated, the strain recovery of the NiTi fibers counteracts the expansion of the aluminum matrix. This combination creates a low density, stiff, and thermally stable material for engineering applications. Previous efforts have shown a 60 % reduction in the average coefficient of thermal expansion for Al 3003 up to 100 C.[3] Yet, metallic bonding between the aluminum matrix and NiTi fibers is not always observed. Instead, the interface is believed to be predominately supported by mechanical coupling in the form of a friction fit.[3] Although metallic bonding is ideal at the interface, mechanical coupling may be sufficient if the interface strength exceeds thermal blocking stresses generated throughout temperature cycling. However, previous efforts have shown evidence of interface failure when significant blocking stresses arise.[4]

To further investigate this high temperature interface failure and build upon interface understanding, a single fiber pullout test was developed to estimate interfacial shear stress.[5] Consequently, by improving understanding of the interface failure characteristics, a more reliable and robust composite can be designed. In addition to estimating the interface strength of current NiTi-Al 6061 composites, the influence of various surface treatments on the NiTi fibers was investigated for possible improvement in the interface strength. The surface treatments investigated were as-built oxide (past surface finish of use and control), chemically etched, mechanically polished, and mechanically roughened. The chemically etched and mechanically polished finish increase the likelihood that metallic bonding may take place due to the as-built oxide layer being removed. On the other hand, the mechanically roughened surface would potentially increase the mechanical interlocking and increase the likelihood of metallic bonding as well. In addition to performing fiber pullout tests, scanning electron microscopy (SEM) and energy dispersive X-ray spectroscopy (EDS) were utilized to compare and contrast bond type and quality for each NiTi surface finish.

2. EXPERIMENTAL METHODS

2.1 Sample Manufacturing

In this study, aluminum 6061-O fully work hardened foil was utilized as the metal matrix for the NiTi-Al UAM composite. Aluminum 6061 was chosen due its frequent use in industry and strong compatibility with VHP-UAM. Samples were manufactured in the Smart Materials and Structures Lab (SMSL) at The Ohio State University on a 9 kW UAM system, Figure 2. The machine is fully automated and includes CNC and laser machining capabilities to complement the additive ultrasonic welding stage.

Figure 2. VHP-UAM system with sonotrode and ultrasonic welder assembly boxed in red.

The NiTi fiber diameter utilized in this study, for all surface finish types, was 0.28 mm (0.011"), and it was purchased from Nitinol Devices Components, Inc. All of the purchased material was trained straight and was super elastic (Austenite finish temperature above room temperature). Welding was performed with a 7 micron Ra surface roughness sonotrode on 101.6 mm by 76.2 mm (4" by 3") aluminum 6061-T6 base plates near 4.76 mm (0.1875") in thickness. The base plates were constrained with a custom metal matrix composite fabrication fixture and vacuum chuck. Foils with a width of 23.81 mm (15/16") and a thickness of 0.152 mm (0.006") were utilized for welding in this experiment. The welding parameters used in this study are presented in Table 1. These parameters were chosen from a recent design of experiment for optimal weld parameters for VHP-UAM of fully work hardened Al 6061-O.[6]

Table 1. Ultrasonic welding parameters used in study.

Parameter	**Value**
Temperature	22°C (70°F)
Force	6000 N
Amplitude	32.76 μm (70%)
Speed	84.6 mm/sec (200 in/min)

To embed the fiber, a 0.3302 mm (0.013") ball end mill was utilized to cut a pocket near 0.254 mm (0.01") deep to aid in fiber placement and encapsulation. The pocket was cut to be slightly undersized to enhace frictional scrubbing on the fiber surface to help promote consolidation. Laser machining was not utilized in this study to minimize aluminum oxide formation in the fiber's pocket prior to embedding. To isolate the fiber, additional machining operations were run intermittent of welding and fiber encapsulation to ensure the embedded fiber was within a representative weld zone of the UAM process. After machining and welding, samples were removed with electrical discharge machining to minimize cutting stresses on the sample and achieve small sample dimensions. Final samples were near 3.175 mm (0.125") in thickness and 22.86 mm (0.9") in width with the NiTi fiber embedded close to center, Figure 3. The fiber length to pull out from the matrix was chosen to be 1 mm (0.04") because fiber strain is transferred to the matrix near the edge of the composite due to shear lag.[5,7] Additionally, this length was chosen for feasible handling during testing.

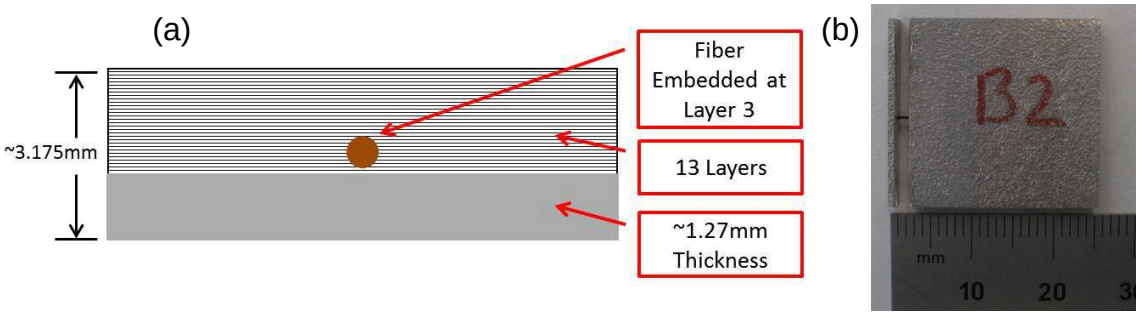

Figure 3. Sample details: (a) schematic of sample cross section with key fabrication details; (b) physical sample ready to test post manufacture.

2.2 Fiber Pullout Testing

Although fiber pullout tests have been detailed in the literature,[5,8,9] no standard has been developed for this type of test. Consequently, a custom fixture was developed and built to fit into square tensile test grips, Figure 4. This test fixture design was inspired and improved from previous interface strength testing of UAM composites at Loughborough University.[10,11] Key features and improvements of this test fixture design are: (i) the ability to load samples by sliding them to center, (ii) a close fit to the samples thickness and the use of closely spaced setscrews to minimize sample misalignment, rotation, and bending, and (iii) an oversized hole drilled at center to minimize fiber misalignment in the testing process. This fixture is made with AISI 1018 Cold Worked Steel to avoid failure and minimize deformation from the fixture.

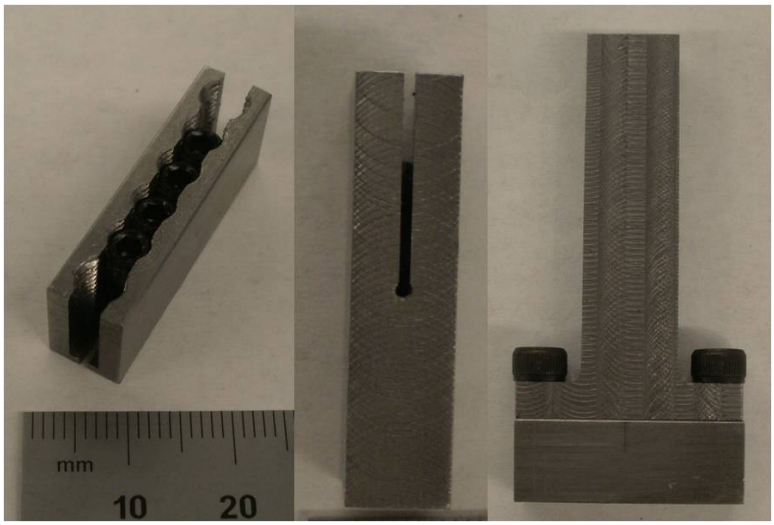

Figure 4. Custom fiber pullout test fixture used in study.

Testing was performed using a TestResources 131R1000-6 load frame with MTS Advantage mechanical wedge type grips and an optional environmental chamber. A detailed test setup can be seen in Figure 5. For testing, a load rate of 1.27 mm/min (0.05 in/min) was applied to the load frame controller once the sample was secured and aligned within the grips. Due to the somewhat fast load rate, a sampling rate of 250 samples/s was utilized to acquire enough data points. Also, the total travel distance was selected to be 2.54 mm (0.1") to ensure that the fiber had completely pulled out of the test fixture before the test was stopped. Measured data included time traces of force and distance for the test.

2.3 Electron Microscopy

In addition to mechanical testing, electron microscopy was performed at The Ohio State University's Center for Electron Microscopy and Analysis (CEMAS) using a FEI Quanta 200 SEM with EDS capability. SEM imaging was done to evaluate consolidation quality and examine the NiTi-Al interface while EDS line scans were performed across various interface regions to quantify diffusion and oxide concentration. Imaging and EDS were done with an electron acceleration voltage of 20 kV, a spot size of 4-5 nm, and a working distance of 12 mm. EDS scan distance was near 15 μm for all samples while sample spacing was near 1 μm. However, the resolution of the EDS is near 4 μm. Consequently, some data smearing occurs near the interface. Finally, each EDS sample point was measured for 20 seconds to fully capture energy states of the atoms of concern.

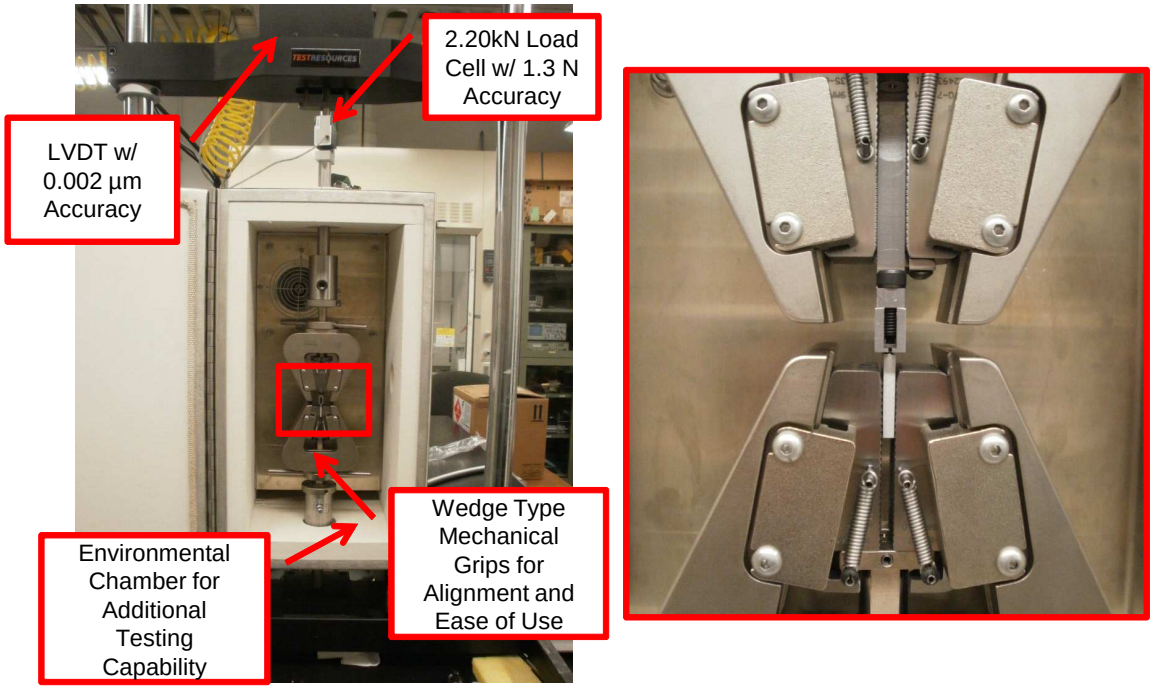

Figure 5. TestResources load frame used in testing with key specifications listed. The area boxed in red illustrates how the test fixture and sample are loaded into the machine.

3. TEST RESULTS

3.1 Fiber Pullout Testing

A representative fiber pullout force-displacement curve and tested oxide surface finish sample can be seen in Figure 6. Key details have been highlighted on the curve to explain test conditions, material behavior, and failure progression. It is emphasized that aluminum remains on the surface of the fiber post failure, which implies matrix rather than interface failure.

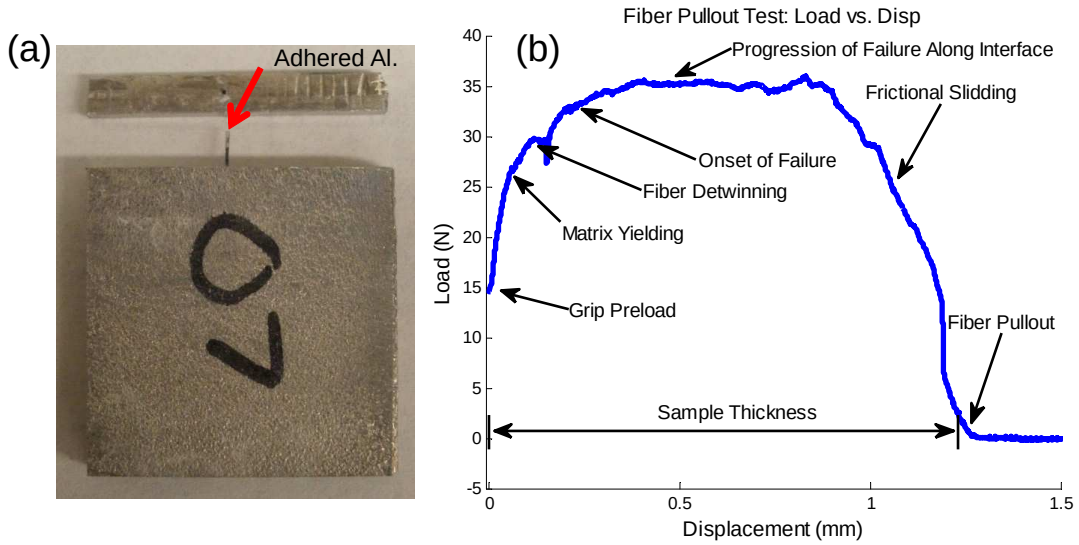

Figure 6. Representative pullout test result for oxide sample 7: (a) photo of sample after failure illustrating adhered aluminum to surface of fiber; (b) detailed force-displacement pullout test curve.

Table 2 summarizes fiber pullout test results for the study. All of the samples failed at a similar load levels while differences in the average shear strength can be observed. The average shear strength was calculated by dividing the peak pullout load by sample thickness. Several of the samples broke during manufacturing or were jeopardized prior to testing and could not be tested or included in the experimental results. However, enough samples were tested to show reasonable consistency amongst a given surface finish.

Table 2. Fiber pullout summary for all surface finishes.

	Oxide	**Roughened**	**Chem. Etched**	**Mech. Polished**
Number of Samples	8	7	3	9
Avg. Peak Pullout Force (N)	37.7	40.5	36.3	37.9
Stdev Peak Pullout Force (N)	5.8	10.7	12.5	9.0
Avg. Sample Length (mm)	1.22	1.02	1.35	1.45
Stdev Sample Length (mm)	0.11	0.20	0.15	0.07
Avg. Shear Stress (MPa)	35.8	45.3	31.1	29.9
Stdev Shear Stress (MPa)	6.7	8.2	12.4	7.5

3.2 Electron Microscopy

SEM images of sample cross sections for each surface finish are presented in Figure 7. These samples were not used in mechanical testing, but were made separately with the same welding conditions as the pullout samples. Tape interfaces cannot be identified easily, which illustrates the consolidation effectiveness of VHP-UAM. Additionally, the Al 6061-T6 base plate material can be identified as the area with the slight contrast difference directly below the fiber. Finally, it can be seen that all the fibers were encapsulated well with some void character. Unexpectedly, some of these voids occur near the bottom of the fiber in the oxide and chemically etched surface finishes compared to the top of the fiber, like the mechanically polished finish. This odd bottom of pocket void characteristic could have originated from contaminants on the fiber surface prior to consolidation, which could limit bonding around the fiber, or the contaminants could promote a corrosive reaction with a chemical utilized in the polishing process.

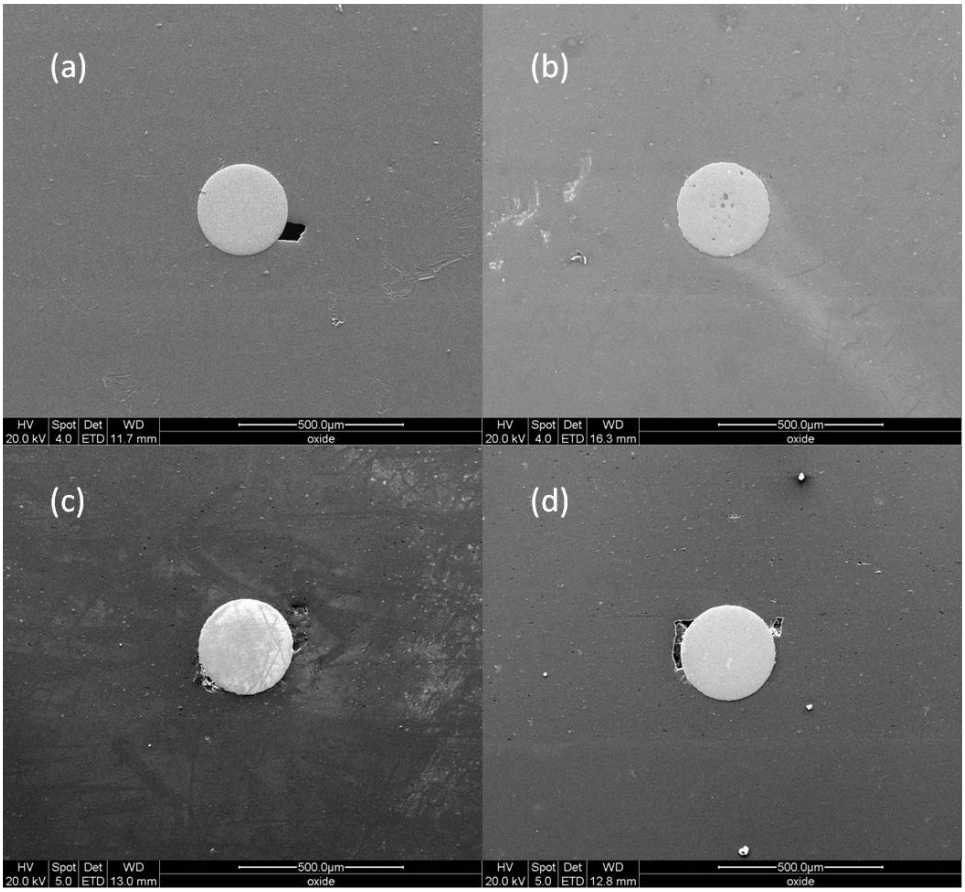

Figure 7. SEM images of embedded NiTi fibers utilized in study: (a) oxide surface finish; (b) mechanically roughened surface finish; (c) chemically etched surface finish; (d) mechanically polished surface finish

EDS line scans with corresponding SEM images for the surface finishes of oxide, roughened, chemically etched, and mechanically polished can be seen in Figures 8–11, respectively. Figure 8 shows a uniform oxide layer near 2 micron in thickness that can be observed in the micrograph and in the EDS line scan. On the other hand, no obvious oxide layer can be observed visually or with EDS for the other surface finishes. However, some oxides do appear to become trapped in the surface roughness of the roughened fiber, as seen in Figure 9. Lastly, for all the surface finishes under investigation, oxygen is observed within the fiber. This oxide is believed to be Titanium Dioxide which formed post sample polishing.

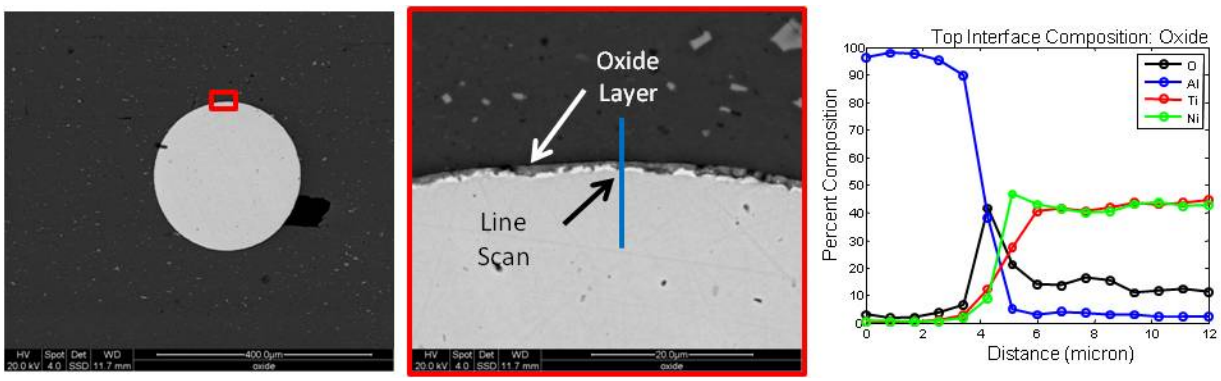

Figure 8. SEM image of top of oxide surface finish fiber with corresponding EDS line scan.

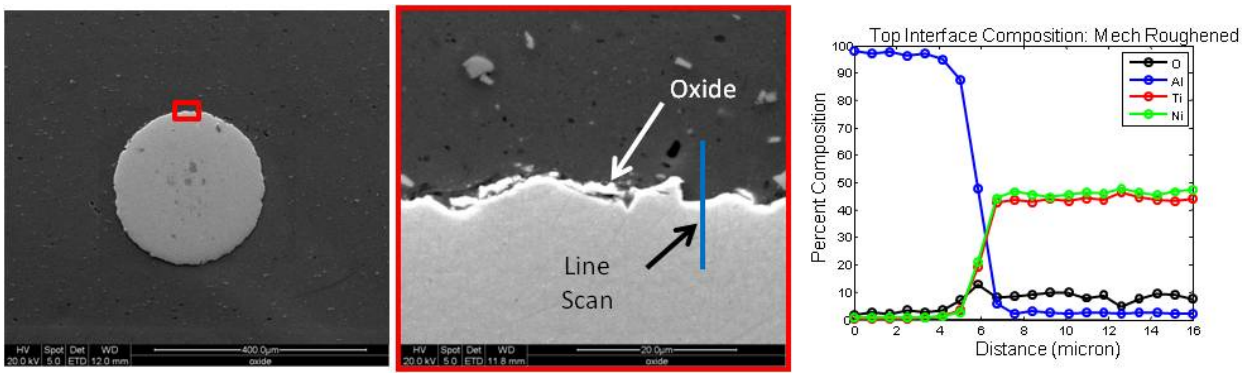

Figure 9. SEM image of top of mechanically roughened surface finish fiber with corresponding EDS line scan.

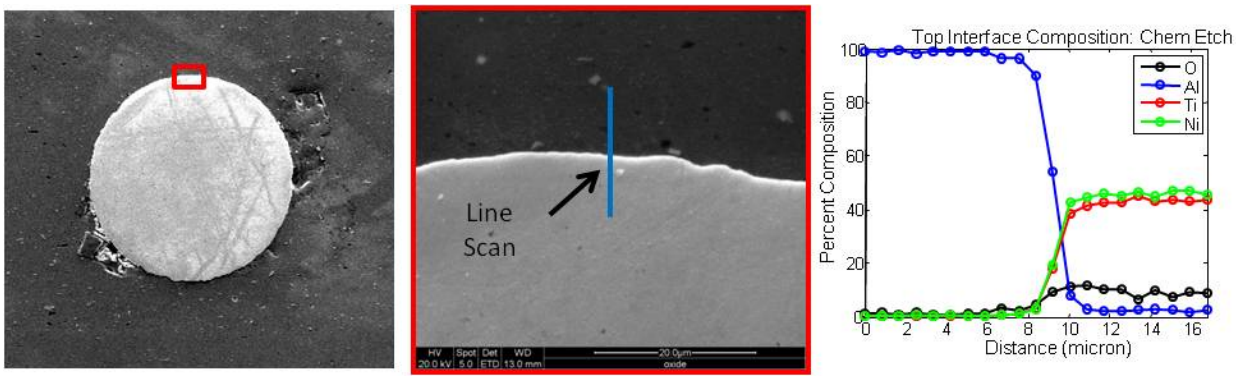

Figure 10. SEM image of top of chemically etched surface finish fiber with corresponding EDS line scan.

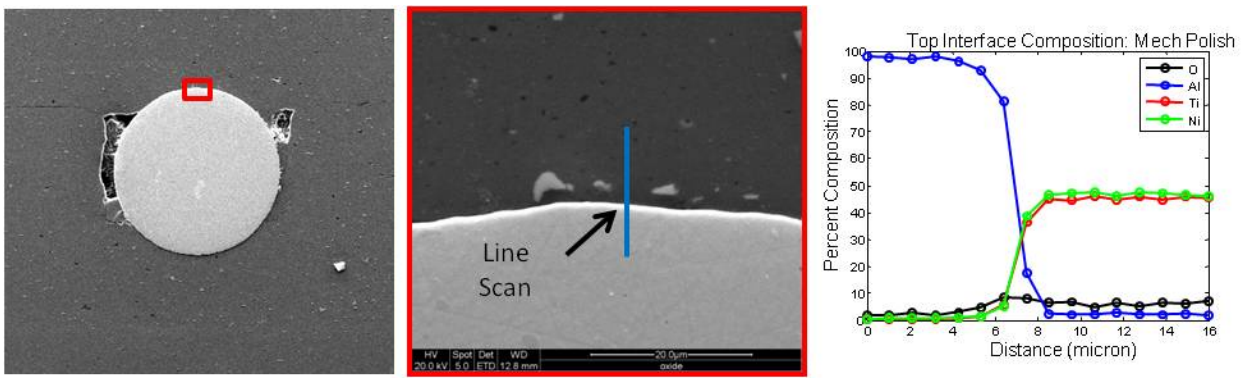

Figure 11. SEM image of top of mechanically polished surface finish fiber with corresponding EDS line scan.

4. DISCUSSION

In order to understand and improve upon the fiber-matrix interface in UAM metal-matrix fiber composites, a fiber pullout test was developed to estimate interfacial shear stress and study failure behavior. In conjunction with developing the fiber pullout test, a finite element model was developed within COMSOL to emulate fiber pullout test conditions on the fiber pullout sample. This FEM model can be seen below in Figure 12 with key details and assumptions. As seen in Figure 12, deformation of the sample is highly localized around the fiber, as desired, to minimize unwanted bending loads.

In addition to using the FEM to analyze sample performance, interface stresses can be estimated from the model to help explain sample failure behavior. Figure 13 illustrates the use of this model to estimate interfacial shear stress for similar conditions observed during testing, specifically a failure load of 40 N and sample thicknesses of 1.0, 1.2, and 1.4 mm respectively. 40 N was chosen as the applied load due to all of the samples failing consistently near this peak load value. As seen in Figure 13, shear stress is concentrated near the edge of the sample and drops off quickly as the fiber length into the matrix increases due to shear lag between the fiber and matrix. As a consequence of this short distance where the load is transferred from the fiber to the matrix, called the critical fiber length,[5] very large localized stresses will be observed, which, in turn, cause failure in a progressive fashion down the fiber. As a result of these large localized stresses and progressive failure behavior, it is expected that failure would occur with the weakest composite element, i.e. matrix, fiber, or interface. Due to the ultimate strength of NiTi being much larger than aluminum, failure is limited to initiate at the interface or matrix.

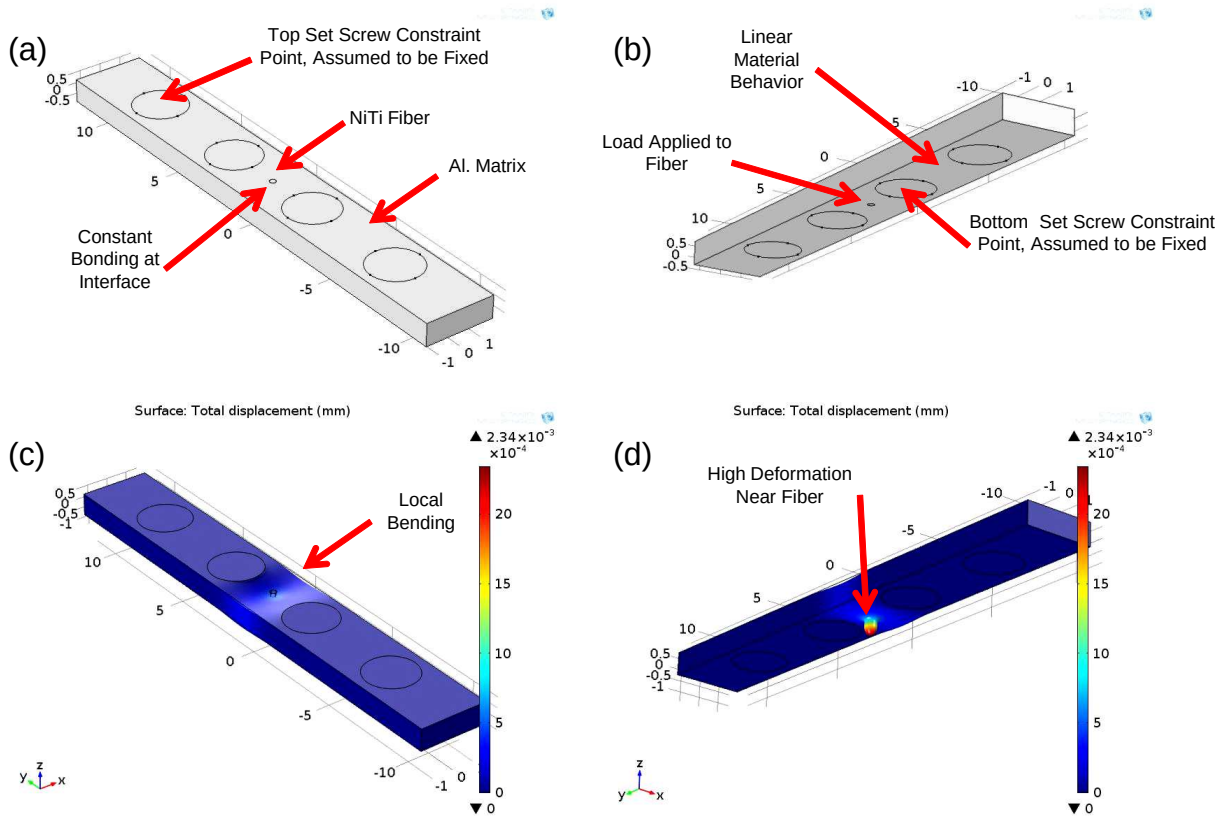

Figure 12. FEM to emulate fiber pullout test conditions with key details: (a) top view of sample; (b) bottom view of sample; (c) displacement view from top of sample; (d) displacement view from bottom of sample.

Table 3 summarizes the average peak stress and average stress of each simulated sample length. The average peak shear stress was calculated by averaging the 3 closest data points to the fiber edge while the average stress utilized all of the data points. The peak stress was averaged due to the exact peak value being difficult to confidently estimate from the stress concentration boundary condition. In addition to comparing the FEM calculations, average empirical shear stress for a given consistent sample length is shown for comparison. From the table, it can be seen that the average peak shear stress is independent of the sample length, which, in turn, correlates well with consistently observed failure loads for all samples and smearing of the average shear stress for longer sample lengths. Additionally, it is noted that the average peak shear stress is near or above the ultimate shear strength of the Al tapes utilized in the UAM process, which explains why failure of the matrix occurs and that remaining Al is consistently observed on pulled out fibers.

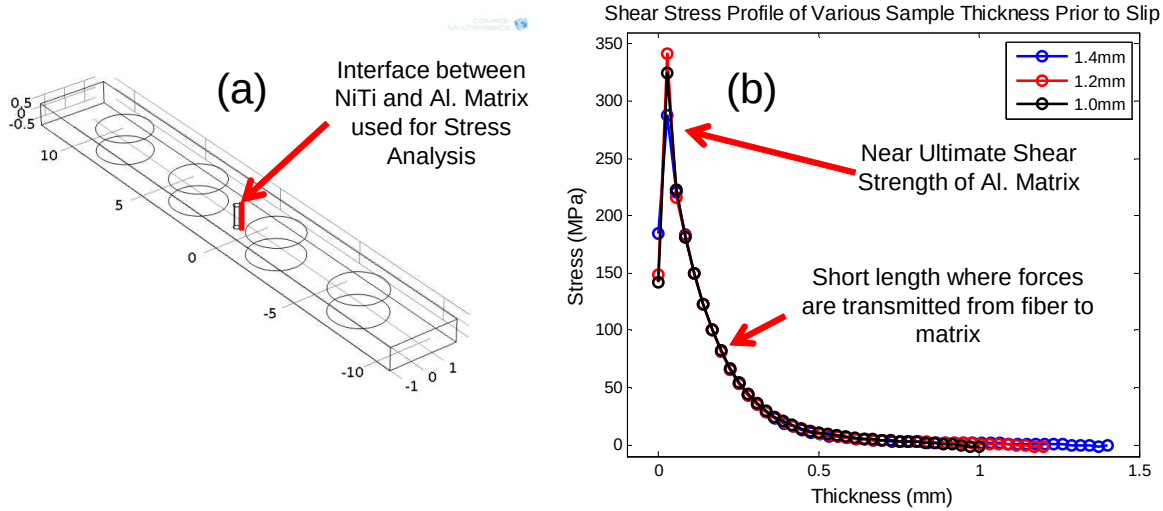

Figure 13. Shear stress analysis of fiber-matrix interface for 40 N load: (a) line in FEM for analysis; (b) shear stress output with key details given for three different sample lengths, similar to lengths used in study.

Table 3. Fiber pullout comparison between FEM and empirical results. Average peak shear stress was computed by averaging first 3 data points near fiber edge while average shear stress averaged all data points over fiber length.

Sample Length (mm)	**Avg. Peak τ(MPa)**	**Avg. FEM τ(MPa)**	**Avg. Empirical τ(MPa)**
1.0	230	46.4	45.3 (Roughened)
1.2	236	39.3	35.8 (Oxide)
1.4	231	33.6	29.9 (Mech. Polished)

In addition to performing fiber pullout tests, electron microscopy was utilized to further understand interface bond mechanisms as a function of surface finish. In general, all fibers demonstrated consolidation quality with little void presence. For the oxide surface finish, it can be confidently said that little to no metallic bonding takes place due to the consistent, unbroken, oxide layer on the fiber. Instead, nearly all interactions between the matrix and fiber would come from friction or mechanical interlocking. On the other hand, the other surface finishes show no observable proof of an oxide layer, which could imply metallic bonding. However, no measurable diffusion is observed at the interface due to the low formation temperature of the UAM process. Consequently, it cannot be confidently said what the exact bond constituents are for the mechanically roughened, chemically etched, or mechanically polished surface finishes.

5. CONCLUSION

In summary, interfacial shear stress and bond mechanisms were studied as a function of NiTi fiber surface finish for NiTi-Al UAM composites with the use of fiber pullout testing and electron microscopy. This study was carried out to improve and understand the Al-NiTi interface for improved design and modeling of NiTi-Al composites due to previous work showing proof of interface failure and frictional bonding between the matrix and fiber. With this study, strong evidence has been shown that the matrix is in fact the weakest link in the composite for all surface finishes due to consistent observation of remaining aluminum on pulled out fibers and simulated peak shear stress being near or above the welded aluminum tape's shear stress. Consequently, bond mechanisms for all fiber surface finishes supersede the strength of the Al matrix and show that there

is no clear optimal surface finish. However, with the use of stronger Al matrices or characterization of the interface at elevated temperatures, surface finish may play a larger role in failure.

Finally, it has been confirmed from previous work that the UAM process is not breaking up the oxide layer on the oxide surface finish fiber and that the bond mechanism is largely a mechanical or a friction fit. While, on the other hand, the other surface finishes have no observable oxide layer that would prohibit metallic bonding. Thus, it is possible that metallic bonding may be taking place. Although the exact bond mechanisms cannot be determined for each fiber, the mechanically roughened fiber appears to be the best from a potential bond strength perspective because it offers both increased frictional coupling and the possibility of metallic bonding.

Acknowledgments

Support for A.H. comes from a National Science Foundation Graduate Fellowship under Grant No. 1102690. Any opinions, findings, and conclusions or recommendations expressed in this material are those of the author(s) and do not necessarily reflect the views of the National Science Foundation. The technical assistance of Phillip Evans (MIT Lincoln Laboratory), Walter Green (OSU), Ross Baldwin (OSU), and Cameron Begg (OSU) is acknowledged.

REFERENCES

[1] Graff, K., [*Ultrasonic Additive Manufacturing*], American Society for Metals International (2011).

[2] Graff, K., Short, M., and Norfolk, M., "Very High Power Ultrasonic Additive Manufacturing (VHP UAM)," in [*International Solid Freeform Fabrication Symposium*], (2011).

[3] Hahnlen, R., *Characterization and Modeling of Active Metal-Matrix Composites with Embedded Shape Memory Alloys*, PhD thesis, The Ohio State University, Columbus, OH (2012).

[4] Hahnlen, R. and Dapino, M., "NiTi-Al Interface Strength in Ultrasonic Additive Manufacturing Composites," *Composites Part B: Engineering* **59**, 101–108 (2014).

[5] Chawla, K., [*Composite Materials: Science and Engineering*], Springer (1998).

[6] Wolcott, P., Hehr, A., and Dapino, M., "Design of Experiment for Optimal Build Parameters for High Power Ultrasonic Additive Manufacturing of Al 6061," in [*SPIE Smart Structures/NDE*], (March 2014).

[7] Li, Z.-F. and Grubb, D. T., "Single-fibre polymer composites: Part i interfacial shear strength and stress distribution in the pull-out test," *Journal of Material Science* **29** (1994).

[8] Marshall, D., Shaw, M., and Morris, W., "Measurement of interfacial debonding and sliding resistance in fiber reinforced intermetallics," *Acta Metallurgica et Materialia* **40**(3) (1992).

[9] Kerans, R. and Parthasarathy, T., "Theoretical analysis of the fiber pullout and pushout test," *Journal of the American Ceramic Society* **74**(7) (1991).

[10] Kong, C., Soar, R., and Dickens, P., "Ultrasonic consolidation for embedding sma fibres within aluminium matrices," *Composite Structures* **66**, 421–427 (2004).

[11] Li, D. and Soar, R. C., "Characterization of Process for Embedding SiC Fibers in Al 6061 O Matrix Through Ultrasonic Consolidation," *Journal of Engineering Materials and Technology* **131** (2009).